Dynamic Control of Nanoprecipitation in a Nanopipette

Boaz Vilozny,[†,‡] Paolo Actis,[†,‡,§] R. Adam Seger,[†,‡] and Nader Pourmand[†,‡,*]

[†]Department of Biomolecular Engineering, University of California Santa Cruz, 1156 High Street, Santa Cruz, California 95064, United States , [‡]Advanced Studies Laboratories, UC Santa Cruz and NASA Ames Research Center, Moffett Field, California 94035, United States, and [§]Department of Biology, Texas Southern University, 3100 Cleburne Street, Houston, Texas 77004, United States

ABSTRACT Studying the earliest stages of precipitation at the nanoscale is technically challenging but quite valuable as such phenomena reflect important processes such as crystallization and biomineralization. Using a quartz nanopipette as a nanoreactor, we induced precipitation of an insoluble salt to generate oscillating current blockades. The reversible process can be used to measure both kinetics of precipitation and relative size of the resulting nanoparticles. Counter ions for the highly water-insoluble salt zinc phosphate were separated by the pore of a nanopipette and a potential applied to cause ion migration to the interface. By analyzing the kinetics of pore blockage, two distinct mechanisms were identified: a slower process due to precipitation from solution, and a faster process attributed to voltage-driven migration of a trapped precipitate. We discuss the potential of these techniques in studying precipitation dynamics, trapping particles within a nanoreactor, and electrical sensors based on nanoprecipitation.

KEYWORDS: nanoprecipitation · nanopipette · nanopore · ion current rectification · current oscillations

Solid state nanopores are of great interest as stable structures that can be used to mimic biological channels,[1] for the size-selective synthesis of nanoparticles,[2] or as nanoscale sensors.[3,4] Conical, or asymmetric, nanopores are a distinct category of nanochannels that display voltage-gated ion current and can behave as nanofluidic diodes.[5,6] Several groups have developed electrical sensors utilizing ion current measurements across membranes containing asymmetric nanopores.[7−11] Such devices are generally prepared by a track-etching method.[12] Glass nanopores fabricated from capillaries can be rapidly prepared using a laser puller.[13] These structures, called nanopipettes, have a conical nanopore at the tip and exhibit many properties of other asymmetric nanochannels. Nanopipettes can be manipulated with high spatial resolution, a property that has been used to image cells at the nanoscale.[14,15] Such conical quartz nanopores have also been functionalized for sensing applications.[16−20]

Investigations with conical nanopores have given rise to new chemical and electrical phenomena that challenge existing ideas about bulk materials. Ion current rectification, the asymmetric enhancement of ion current as a voltage is applied across an electrolyte-filled nanopore, has been well documented.[21] Recently, ion current oscillations were observed with rectifying conical nanopores (2−8 nm diameter) in polyethylene terapthalate (PET) films, and were attributed to dynamic precipitation in the pore caused by voltage-induced concentration of weakly soluble salts.[22,23] Current oscillations in much larger pores of silicon nitride or borosilicate glass can be generated at the interface of two solvents using organic molecules with differential solubility.[24] These phenomena offer a new way to electrically monitor nonequilibrium events such as precipitation in real time and at the nanoscale. We now report on the phenomenon of voltage-dependent current oscillations arising from precipitation of zinc phosphate, a salt with extremely low water solubility, at the pore of a quartz nanopipette.

In this report, we demonstrate how a voltage bias across a nanopipette opening can be employed to control ion migration and cause precipitation of an insoluble salt at the interface of two aqueous media. Furthermore, we describe the conditions required to generate oscillating current due to zinc phosphate precipitation in a nanopore, as well as investigations into the nature of the precipitate and its subsequent evacuation from the pore. We also demonstrate that a pore which appears permanently blocked by precipitation can be briefly cleared with a voltage pulse, and we use this method to examine the kinetics of pore blockage.

RESULTS AND DISCUSSION

To use the nanopipette as a nanoreactor, we established conditions to control the precipitation of zinc phosphate at the pore through ion migration. In a typical setup, an Ag/AgCl electrode is inserted into an electrolyte solution (100 mM KCl with 10 mM buffer) that fills the barrel of a nanopipette.

* Address correspondence to pourmand@soe.ucsc.edu.

Received for review January 25, 2011 and accepted March 17, 2011.

Published online March 17, 2011
10.1021/nn200320b

The nanopipette tip is immersed in an electrolyte bath, which also contains an Ag/AgCl ground electrode (Figure 1a). On applying a potential, a steady ion current is measured. However, on adding micromolar concentrations of zinc chloride to the bath, the system undergoes oscillating periods of high and low conductance. We attribute these cycles to precipitation of highly insoluble zinc phosphate inside the nanopipette tip (Figure 1b), and its subsequent evacuation from the pore.

The oscillations caused by nanoprecipitation in such nanopipettes are on the order of seconds, as shown in Figure 1c, and are marked by a fluctuating state of low conductance and rapid, short-lived oscillations to a state of high conductance. The time plot of the ion current at −350 mV potential shows several precipitation events that do not terminate with complete opening of the pore; rather, there are many events in which the low-conductance state fluctuates between −400 and −700 pA. These are likely due to precipitates that are evacuated before they grow to a size sufficient to completely block the pore. When a state of high conductance is reached, however, the current consistently reaches a maximum value of roughly −1200 pA followed by a rapid drop to −400 pA. This indicates a complete clearing of the pore followed by rapid precipitation.

It is important to show that the precipitation reaction is controlled by the voltage-induced ion migration of zinc and phosphate ions, and does not simply occur by mixing at the nanopore, which is the interface of the two solutions. We isolated the zinc and phosphate counterions in two separate solutions; phosphate ions are confined to the inside of the nanopipette, and zinc ions are in the bath (Figure 1a). The minimum required voltage to induce oscillating current blockage in this system is −300 mV. At potentials from +500 mV to −200 mV, a stable current is seen. At −300 mV, the current immediately becomes blocked with rapid fluctuations (see Supporting Information, Figure 1). The existence of a voltage threshold for the nanoprecipitation reaction indicates there is little mixing between the two counterions at the interface of the two solutions. Applying a positive potential gives a signal of smaller magnitude due to current rectification, but the signal is not influenced by the presence of zinc or phosphate salts. This voltage-dependent effect is consistent with the movement of ions toward the electrode of opposite charge, with phosphate and zinc ions meeting at the pipet tip (Figure 1b). When the placement of solutions is reversed such that zinc chloride is inside the nanopipette barrel and phosphate is in the bath, no blockage occurs with either a positive potential or a negative potential. While a positive potential in this configuration can in theory cause precipitation as zinc ions are pushed out of the pore and phosphate migrates into the pore from the bath, this is not observed. The lack of current blockage in this configuration may be due to exclusion of cations (such as zinc) at the inner tip of the pore, a phenomenon often cited as a cause of current rectification in conical nanopores.[13]

The current oscillations due to nanoprecipitation raise several questions about the nature of the precipitate, the role of applied voltage in precipitation, and the subsequent clearing of the precipitate from the pore. We assume the precipitate is composed of zinc phosphate, a salt which is highly insoluble in aqueous systems ($K_{sp} = 10^{-35}$).[25] While the predominant species in solution at pH 7 are dihydrogen phosphate ($H_2PO_4^-$) and hydrogen phosphate (HPO_4^{2-}), zinc phosphate is thermodynamically stable and forms in solutions at neutral or acidic pH.[26] A solution is saturated with roughly 1×10^{-7} M phosphate and zinc ions. Oscillating current behavior was seen in pipettes filled with phosphate buffer from pH 6 to pH 10, and with zinc chloride added to the bath at concentrations between 2 and 40 μM. While other divalent ions such as calcium and magnesium were tested at those concentrations, the only other comparable blockage was with iron(III) chloride (10 μM), which irreversibly blocked the pore. This is likely due to iron(III) hydroxide precipitation, a salt even less soluble than zinc phosphate (K_{sp} $Fe(OH)_3 = 10^{-39}$).[27]

There are several possible mechanisms by which a nanopore blocked by precipitation spontaneously becomes cleared. For current oscillations seen with phosphate salts of calcium and cobalt in PET track-etched nanopores, the precipitation was attributed to voltage-induced concentration of salts in an asymmetric nanopore, causing a local increase in salt concentration to supersaturation levels.[23] This led to a hypothesis in which the precipitate rapidly dissolves due to ion depletion in the nanopore. A computational study supported a second mechanism, wherein protons donated by hydrogen phosphates in the precipitate are accepted by oxides at the pore surface, weakening the pore−particle interaction and allowing the particle to clear by migration.[28] For the pore blockage reported here, the effect is only observed at concentrations between 1 and 100 μM zinc chloride, well above the saturation level for zinc phosphate. Thus, the latter mechanism of particle migration offers an explanation for the oscillations observed here. To support this mechanism, we induced current oscillations in a pipet filled with phosphate buffer and immersed in a saturated solution of zinc phosphate. The precipitate in such a case is likely ejected from the pore, rather than dissolved (see Figure 2).

If the zinc phosphate precipitate migrates out from the pore as we believe, it remains to be explained why current oscillations are seen only with negative potentials. While the exact chemical composition of the precipitate is unknown at this time, clusters of zinc phosphate have been shown to have a net negative

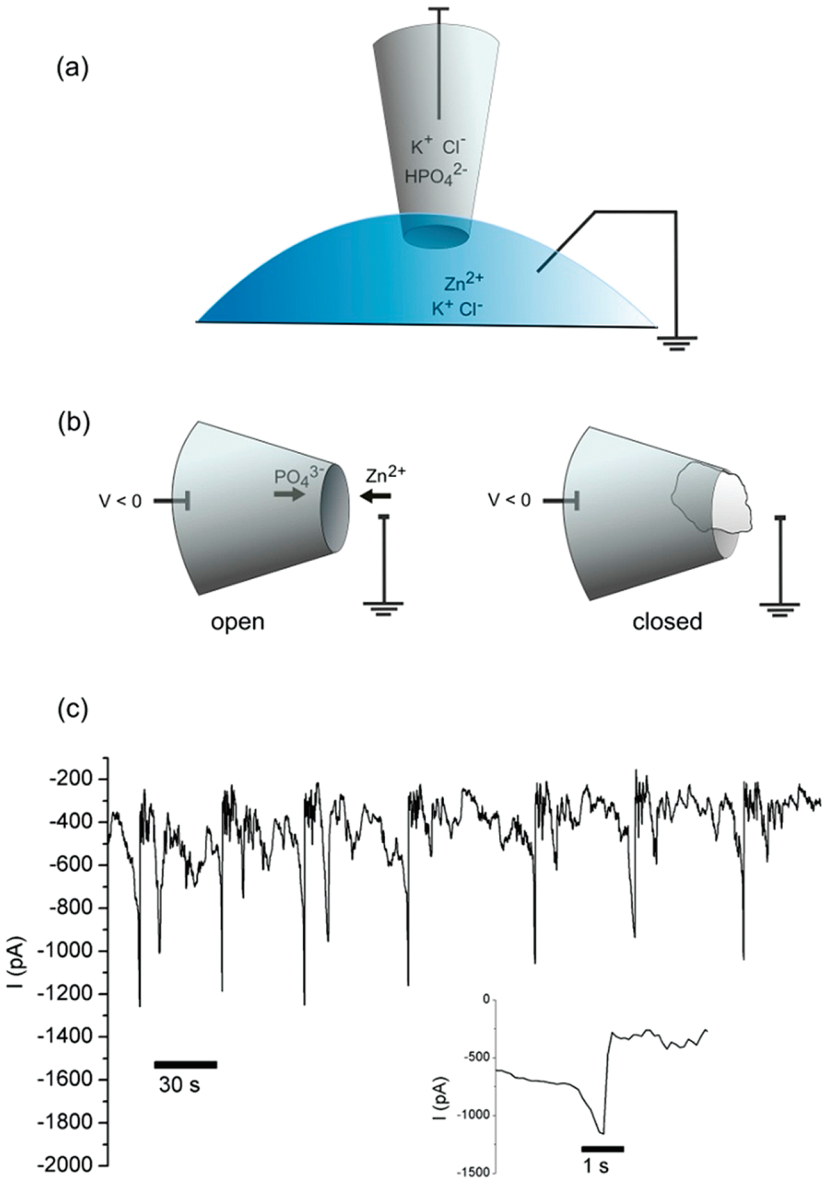

Figure 1. Measurement of ion current oscillations in a nanopipette. (a) Electrochemical setup to measure ion current through a quartz nanopipette with pore diameter 40−60 nm. All solutions contain KCl (0.1 M) and are buffered at pH 7, with 10 mM potassium phosphate in the barrel and 10 mM Tris-HCl in the bath. Zinc chloride is included in the bath at concentrations of 2−20 μM. (b) Configuration causing ion current oscillations. A negative potential in the nanopipette barrel draws zinc cations from the bath into the pore while phosphate ions are pushed out into the bath. When a precipitate of sufficient size is formed, the pore is blocked and ionic current decreases. (c) Current oscillations in a nanopipette setup with 2 μM zinc chloride in the bath and a potential of −350 mV. Inset: expanded view of one of the open states.

charge at neutral pH, as measured by zeta potential.[29] Precipitation and blocking of the pore will lead to an increased electric field at the pore, and thus a negative potential may move the precipitate out of the pore and into the bath by electrophoretic forces. While the applied voltages are low in these experiments (−300 to −500 mV), the voltage drop will be greatest across the region of highest impedance, such as the blocked pore. Thus, a negatively charged particle will only be ejected once it has grown to sufficient size to block the pore, increasing the local electric field and the force on the particle. Ejection of the particle by electrophoretic forces may also help to explain why iron(III)hydroxide does not exhibit spontaneous clearing from the pore, as the particles carry a positive charge[30] and would be expected to have a strong interaction with the negatively charged quartz surface. Interestingly, a pipet showing positive current rectification after deposition of a poly-L-lysine electrolyte layer[31] became blocked from voltage-induced mixing of zinc phosphate, but did not display any oscillations to an open state. Presumably, the negatively charged precipitate has a high affinity for a positively charged pore and cannot be dislodged as easily.

Controlled precipitation in a nanoreactor may include controlling the size of the precipitate. If the pore

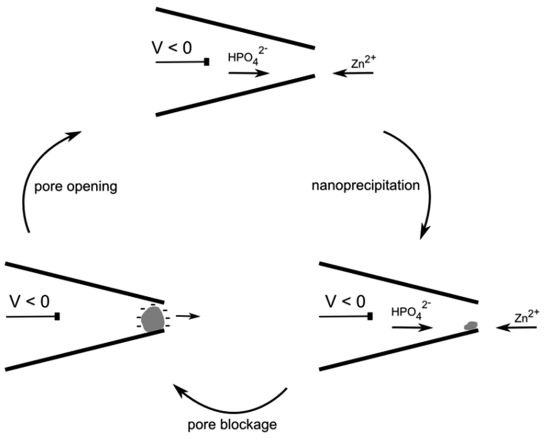

Figure 2. Oscillations in ion current by clearing of precipitate from the pore. With a negative potential, oppositely charged ions migrate to the interface of the solutions inside and outside the pipet. Zinc phosphate precipitates at the pore, causing ion current to decrease. When the precipitate has grown to sufficient size, it is cleared from the pore by electrophoretic forces.

is cleared due to electrical forces acting on charged particles at the tip of the nanopipette, then increasing the potential is expected to eject smaller particles that have not completely blocked the pore. This was demonstrated experimentally by analyzing current oscillations occurring with potentials from −300 to −600 mV. At a potential of −600 mV, two distinct low-conductance states are seen which may correspond to ejection of two sizes of particles (Figure 3a).

A histogram of ion current levels shows a state of high and low conductance for −300, −400, −500, and −600 mV. At −600 mV, there is clearly more time spent in the open state relative to the closed state, also visible in the time plot (Figure 3a). For example, the system at −300 mV shows 41% time spent in a high conductance state, while at −600 mV, that value is 73%. This indicates that as the potential increases, the precipitate is prevented from blocking the pore. Unlike the other voltages measured, the time plot at −600 mV shows three states: a low conductance state (−800 pA) that occurs infrequently and for longer duration than an intermediate state (−3000 to −3500 pA), and a high conductance state (−6000 pA). We believe the intermediate state corresponds to precipitates that are ejected by the higher electric field before they have grown sufficiently to block the pore. At voltages less than −600 mV, the precipitate is cleared only after it has grown to sufficient size to completely block the pore.

It is expected that at some point salt will accumulate in the conical pore to an extent that the precipitate cannot be ejected. This stage of precipitation was also studied with the nanoreactor, and revealed an unforeseen phenomenon. Many of the nanopipettes underwent three stages of blocking by nanoprecipitation. The first stage was that of spontaneous current oscillations with a constant negative applied potential. After a period of 20 min or more, the pore became blocked and exhibited a steady state of low-conductance. At this stage, however, the pore could be temporarily forced into a high-conductance state by a rapid pulse of positive potential. Finally, the pipet would become irreversibly blocked. For the first two stages, we sought to understand what was occurring in the nanopipette as the pores are becoming cleared and subsequently blocked. The kinetics of pore opening cannot be compared for the two systems, as they occur under potentials of opposite polarity. We investigated the kinetics of pore closing to find if there are different mechanisms at work for a pipet in the two stages described.

If the pore can be cleared by a negative potential causing migration of a negatively charged particle out through the nanopore, then a positive potential is expected to move the precipitate in the opposite direction, to the broader shaft of the nanopipette. For blocked pores, a pulse of +500 mV was briefly applied (0.2−2 s), followed by reversal of the voltage to −500 mV. At the negative voltage, a high conductance state is seen from the previously blocked pore, which again becomes rapidly blocked (Figure 4a). The brief open state is of the same magnitude as the open states in nanopipettes undergoing current oscillations, and is therefore attributed to an open pore rather than a transient current due to the rapid change in voltage. The temporary high-conductance state followed by pore closing indicates that the precipitate has migrated away from the pore and is either replaced by precipitation from solution, or that the particle is moved back toward the pore when the potential is reversed from positive to negative.

The kinetics of pore closing will be distinct for the two different mechanisms, nanoprecipitation *versus* migration of a particle into the pore. To compare blocking kinetics in oscillating *versus* blocked pores, we quantified the rate of current blockage for individual events at −500 mV for both conditions. For blocked pores that have been briefly opened with a +500 mV pulse, the current for a blocking event decreases with a slope of 74 ± 13 pA/ms, as compared to 4 ± 2 pA/ms for a pore undergoing current oscillations. The significantly faster current blockage indicates a blocking mechanism other than nanoprecipitation from solution. Rather, this may represent voltage-driven shuttling inside the nanopipette, from base to tip, of a particle too large to exit through the nanopore. This phenomenon has thus far only been observed with zinc phosphate salts, and did not occur with blockage from other precipitates such as iron(III)hydroxide.

If the precipitate in a blocked nanopipette is indeed moved within the nanopipette tip during pulses of positive potential, then the particle can be trapped between base and tip of the conical pore with alternating voltages. By applying sinusoidal potentials of sufficiently high frequency, an "open" current can be produced from

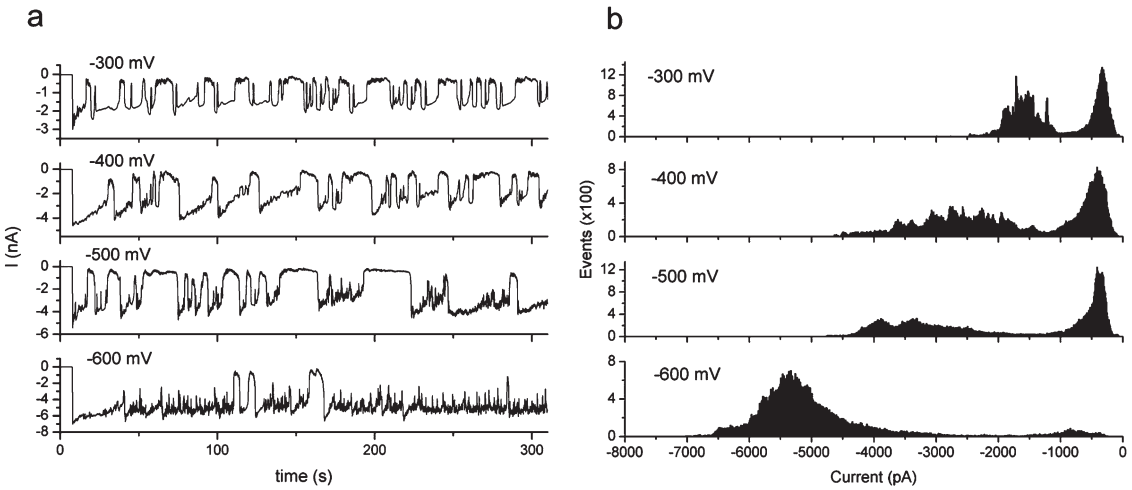

Figure 3. Voltage-dependence of current oscillations; (a) oscillations on applying a negative potential to a pipet filled with phosphate buffer (pH 7) and immersed in a bath of Tris-HCl buffer (pH 7) with 2 μM zinc chloride; (b) histograms showing events in the states of high and low conductance.

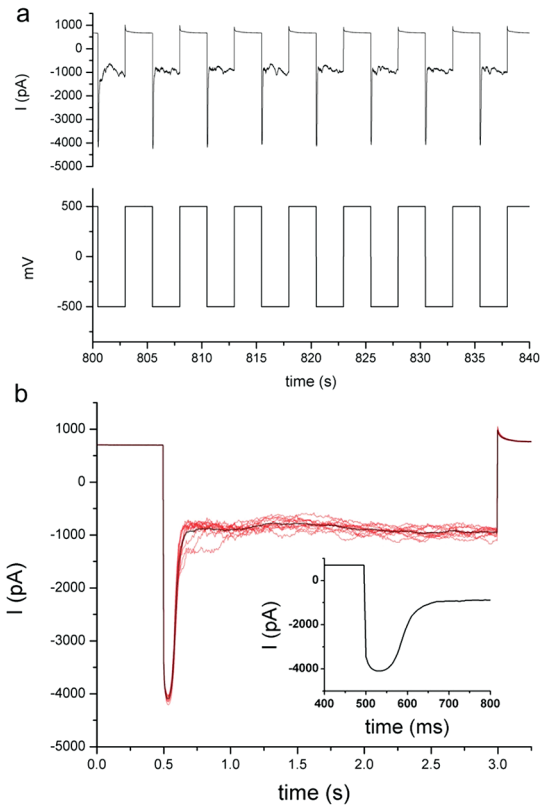

Figure 4. Kinetics of voltage-driven pore clearing: (a) a pore that has become blocked due to nanoprecipitation can be temporarily cleared by applying a pulse of positive potential; (b) the plot shows the average of several such events (N = 11). Inset: Kinetics of pore blockage after temporary opening. The pipet was filled with pH 7 phosphate buffer (10 mM phosphate and 100 mM KCl) and immersed in pH 7 Tris buffer (10 mM Tris and 100 mM KCl) with 2 μM zinc chloride.

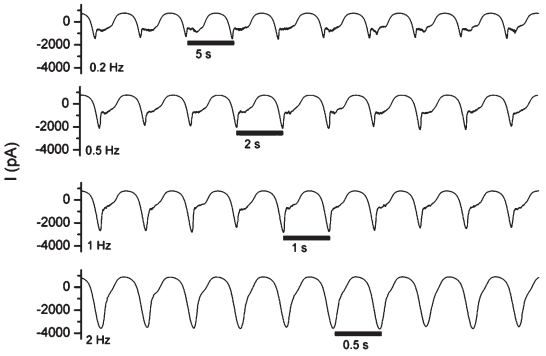

Figure 5. Response of a blocked pipet to frequency of applied potential. A pipet filled with pH 7 phosphate buffer (10 mM with 100 mM KCl) was immersed into a bath of pH 7 Tris buffer (10 mM with 100 mM KCl) containing 2 μM zinc chloride. The pipet became blocked after constant potential of −500 mV for several minutes, and sinusoidal potential from 500 to −500 mV was applied at frequencies of 0.2, 0.5, 1, and 2 Hz.

pipettes which appear to be blocked by zinc phosphate (Figure 5). At lower frequencies such as 0.1 Hz, the pore can be seen to briefly approach a high-conductance state before becoming blocked as the potential oscillates to a negative voltage. At higher frequencies a much higher conductance state is achieved, as the particle is not subjected to an electric field for sufficient time to migrate to the tip. Notably, the magnitude of current during the high-frequency voltage wave (−3500 pA) is similar to that when the voltage is instantly switched from +500 to −500 mV (Figure 4). In both cases, we believe the negative current can only be briefly sustained before the pore is again blocked by electrophoretic movement of the particle to the nanopipette tip.

With higher frequencies of voltage (2 Hz) the particle is prevented from reaching the tip. With slower frequencies of sinusoidal voltage (0.2 Hz), the particle migrates to the tip before the potential reaches −500 mV and the system cannot achieve a high-conductance state. The high-conductance state achieved with higher frequencies of sinusoidal voltage represents

trapping in space of a nanoprecipitate using an oscillating electric field, and also allows the magnitude of current to be precisely controlled with frequency of the applied potential.

CONCLUSIONS

In this work, electrical techniques were used to induce and monitor precipitation events taking place in a pore of less than 100 nm diameter. We conclude from these experiments that voltage-controlled ion migration is an effective way to investigate chemical reactions using nanomaterials. The nanoscale opening of the quartz pipettes offers a high level of sensitivity to precipitation that may not be observed with other techniques. While the results shown here are for highly insoluble zinc phosphate salts, reports of precipitation in pores less than 10 nm with more soluble salts[22,23] indicate that similar experiments can be carried out with a variety of ions. Future work will address how the pore dimensions, as well as factors such as ionic strength and pH, affect the ability to induce and detect such precipitation events. Investigations into the exact nature of the precipitate, the kinetics of such current oscillations, and interactions with other solutes are also the subject of ongoing experiments.

The ability to control and measure the kinetics of salt precipitation at the nanoscale may lead to new techniques for studying dynamic processes such as biomineralization and dissolution. The trapping of a precipitate within the nanoreactor by voltage oscillations may be a future tool to study size and surface charge of nanoparticles. The controlled nanoprecipitation of insoluble salts may also be valuable in developing selective and sensitive ion sensors. The reaction shown here was able to detect as little as 2 μM zinc chloride and was unaffected by the presence of other cations such as potassium or magnesium. Furthermore, the ability for a pore blocked by precipitation to be opened through oscillating potentials can expand the applications for sensing with nanopores. For example, a constant voltage may be used to detect nanoprecipitation, while oscillating potentials can be used to measure ion current for other sensing applications.

METHODS

Reagents and Solutions. Stock solutions of metal salts (100 to 500 mM) were prepared in Milli-Q ultrapure water with 5% HCl. These were then diluted in buffer the day of the experiment. Calcium chloride tetrahydrate was purchased from Fisher. Zinc chloride, iron(III) chloride, and magnesium chloride (1.00 M solution) were purchased from Sigma-Aldrich. Buffer solutions were prepared from potassium chloride (Baker), sodium phosphate, dibasic (Sigma), and TRIS-HCl (1 M solution, pH 7.00, Sigma) and adjusted with either HCl (1 M) or KOH (0.1 M). All buffer solutions used for analysis contained 10 mM buffer and 100 mM potassium chloride.

Quartz Nanopipette Fabrication. Nanopipettes were fabricated from quartz capillaries with filaments, with an outer diameter of 1.0 mm and an inner diameter of 0.70 mm (QF100-70-5; Sutter Instrument Co.). The capillary was then pulled using a P-2000 laser puller (Sutter Instrument Co.) preprogrammed to fabricate nanopipettes with an inner diameter of approximately 50 nm.[32] Parameters used were as follows: Heat 625, Filament 4, Velocity 60, Delay 170, and Pull 180. In a solution of 10 mM buffer and 100 mM KCl, the pipettes gave a current between −2500 and −4000 pA at a potential of −0.5 V.

Measurement Setup. For measuring ionic current through a nanopipette, a two-electrode setup was used. The nanopipette was backfilled with buffer solution and an Ag/AgCl electrode inserted. Another Ag/AgCl electrode was placed in 0.3 mL of bulk solution acting as auxiliary/reference electrode. Both electrodes were connected to an Axopatch 700B amplifier with the DigiData 1322A digitizer (Molecular Devices), and a PC equipped with pClamp 10 software (Molecular Devices). Positive potential refers to anodic potential applied to the electrode in the barrel of the pipet relative to the counter electrode. Experiments were carried out at 24 °C.

Voltage-Driven Nanoprecipitation. To induce zinc phosphate precipitation by voltage-driven mixing, the barrel of a nanopipette was backfilled with a solution of phosphate buffered electrolyte, and the tip immersed in a phosphate-free Tris-HCl buffer. An aliquot of zinc chloride solution was added to the bath and stirred by repeated pipetting. The system was monitored while applying voltages from +500 to −800 mV. Experiments at different pH varied the phosphate buffer in the barrel only, with pH values of 6, 7, 8, or 10.

Kinetics of Current Oscillations. Nanopipettes were selected with a current value of −3500 to −4500 pA at a potential of −500 mV. Potentials from −300 to −500 mV produced current oscillations, for which a threshold was set for high and low conductance states. By measuring the time from high to low conductance, the slope of pore closing was estimated in pA per ms. The high and low conductance states were set as follows: −500 mV, −1700 and −1200 pA; −400 mV, −1200 and −700 pA; −350 mV, −900 and −400 pA; −300 mV, −1000 and −500 pA. For temporary opening of the pore, a biphasic waveform was used, where the applied potential oscillated between +500 and −500 mV for a period of 2.5 s each. The threshold for high conductance was set at −3500 pA, and the low conductance state at −2000 pA. The slope was calculated from the time required to reach the low conductance state.

Data Analysis. Data was sampled at a rate of 1 kHz using Clampex software. Data processing was done using Clampfit and OriginPro 8.5 (OriginLab, Northhampton, MA). Calculation of relative time in high *versus* low conductance states used the peak finding function of OriginPro to find either negative (high conductance) or positive (low conductance) peaks, and the number of events in each state calculated as a percentage of the total events.

Acknowledgment. This work was supported in part by grants from the National Aeronautics and Space Administration Cooperative Agreements NNX10AQ16A and NNX08BA47A, and the National Institutes of Health [P01-HG000205].

Supporting Information Available: One figure showing the voltage threshold for nanoprecipitation; one figure showing blockage of a pore functionalized with poly-L-lysine. This material is available free of charge *via* the Internet at http://pubs.acs.org.

REFERENCES AND NOTES

1. Dekker, C. Solid-State Nanopores. *Nat. Nanotechnol.* **2007,** *2*, 209–215.
2. Guo, P.; Martin, C. R.; Zhao, Y. P.; Ge, J.; Zare, R. N. General Method for Producing Organic Nanoparticles Using Nanoporous Membranes. *Nano Lett.* **2010,** *10*, 2202–2206.

3. Howorka, S.; Siwy, Z. Nanopore Analytics: Sensing of Single Molecules. *Chem. Soc. Rev.* **2009,** *38*, 2360–2384.
4. Siwy, Z. S.; Davenport, M. Biosensors: Making Nanopores from Nanotubes. *Nat. Nanotechnol.* **2010,** *5*, 174–175.
5. Cheng, L. J.; Guo, L. J. Nanofluidic Diodes. *Chem. Soc. Rev.* **2010,** *39*, 923–938.
6. Siwy, Z. S.; Howorka, S. Engineered Voltage-Responsive Nanopores. *Chem. Soc. Rev.* **2010,** *39*, 1115–1132.
7. Harrell, C. C.; Choi, Y.; Horne, L. P.; Baker, L. A.; Siwy, Z. S.; Martin, C. R. Resistive-Pulse DNA Detection with a Conical Nanopore Sensor. *Langmuir* **2006,** *22*, 10837–10843.
8. Kececi, K.; Sexton, L. T.; Buyukserin, F.; Martin, C. R. Resistive-Pulse Detection of Short dsDNAs Using a Chemically Functionalized Conical Nanopore Sensor. *Nanomedicine (London)* **2008,** *3*, 787–796.
9. Sexton, L. T.; Horne, L. P.; Martin, C. R. Developing Synthetic Conical Nanopores for Biosensing Applications. *Mol. Biosyst.* **2007,** *3*, 667–685.
10. Ali, M.; Schiedt, B.; Neumann, R.; Ensinger, W. Biosensing with Functionalized Single Asymmetric Polymer Nanochannels. *Macromol. Biosci.* **2010,** *10*, 28–32.
11. Siwy, Z.; Jan, B.; Fertig, N.; Fulinski, A.; Martin, C. R.; Neumann, R.; Trautmann, C.; Molares, E. T. Nanodevice for Controlled Charged Particle Flow and Method for Producing Same. U.S. Patent 7,708,871, September 24, 2003.
12. Spohr, R.; Apel, Y. P.; Korchev, Y.; Siwy, Z.; Yoshida, M., Method for Etching at least One Ion Track to a Pore in a Membrane and Electrolytic Cell for Preparing said Membrane. U.S. Patent 7,001,501, March 6, 2003.
13. Wei, C.; Bard, A. J.; Feldberg, S. W. Current Rectification at Quartz Nanopipet Electrodes. *Anal. Chem.* **1997,** *69*, 4627–4633.
14. Ying, L. M. Applications of Nanopipettes in Bionanotechnology. *Biochem. Soc. Trans.* **2009,** *37*, 702–706.
15. Klenerman, D.; Korchev, Y. Potential Biomedical Applications of the Scanned Nanopipette. *Nanomedicine (London)* **2006,** *1*, 107–114.
16. Sa, N.; Fu, Y.; Baker, L. A. Reversible Cobalt Ion Binding to Imidazole-Modified Nanopipettes. *Anal. Chem.* **2010,** *82*, 9963–9966.
17. Fu, Y.; Tokuhisa, H.; Baker, L. A. Nanopore DNA Sensors Based on Dendrimer-Modified Nanopipettes. *Chem Commun (Cambridge)* **2009,** 4877–4879.
18. Umehara, S.; Karhanek, M.; Davis, R. W.; Pourmand, N. Label-Free Biosensing with Functionalized Nanopipette Probes. *Proc. Natl. Acad. Sci. U.S.A.* **2009,** *106*, 4611–4616.
19. Actis, P.; Mak, A.; Pourmand, N. Functionalized Nanopipettes: Toward Label-free, Single Cell Biosensors. *Bioanal. Rev.* **2010,** *1*, 177–185.
20. Actis, P.; Jejelowo, O.; Pourmand, N. Ultrasensitive Mycotoxin Detection by STING Sensors. *Biosens. Bioelectron.* **2010,** *26*, 333–337.
21. Cervera, J.; Schiedt, B.; Neumann, R.; Mafe, S.; Ramirez, P. Ionic Conduction, Rectification, and Selectivity in Single Conical Nanopores. *J. Chem. Phys.* **2006,** *124*, 9.
22. Innes, L.; Powell, M. R.; Vlassiouk, I.; Martens, C.; Siwy, Z. S. Precipitation-Induced Voltage-Dependent Ion Current Fluctuations in Conical Nanopores. *J. Phys. Chem. C* **2010,** *114*, 8126–8134.
23. Powell, M. R.; Sullivan, M.; Vlassiouk, I.; Constantin, D.; Sudre, O.; Martens, C. C.; Eisenberg, R. S.; Siwy, Z. S. Nanoprecipitation-Assisted Ion Current Oscillations. *Nat. Nanotechnol.* **2008,** *3*, 51–57.
24. Yusko, E. C.; Billeh, Y. N.; Mayer, M. Current Oscillations Generated by Precipitate Formation in the Mixing Zone Between Two Solutions Inside a Nanopore. *J. Phys.: Condens. Matter* **2010,** *22*, 454127.
25. Kanzaki, N.; Onuma, K.; Treboux, G.; Tsutsumi, S.; Ito, A. Inhibitory Effect of Magnesium and Zinc on Crystallization Kinetics of Hydroxyapatite (0001) Face. *J. Phys. Chem. B* **2000,** *104*, 4189–4194.
26. Nriagu, J. O. Solubility Equilibrium Constant of Alpha-Hopeite. *Geochim. Cosmochim. Acta* **1973,** *37*, 2357–2361.
27. CRC *Handbook of Chemistry and Physics*, 91 ed.; Taylor and Francis: Oxford, UK, 2010.
28. Cruz-Chu, E. R.; Schulten, K. Computational Microscopy of the Role of Protonable Surface Residues in Nanoprecipitation Oscillations. *ACS Nano* **2010,** *4*, 4463–4474.
29. Herschke, L.; Lieberwirth, I.; Wegner, G. Zinc Phosphate as Versatile Material for Potential Biomedical Applications Part II. *J. Mater. Sci.-Mater. Med.* **2006,** *17*, 95–104.
30. Davis, C. C.; Chen, H.-W.; Edwards, M. Modeling Silica Sorption to Iron Hydroxide. *Environ. Sci. Technol.* **2001,** *36*, 582–587.
31. Umehara, S.; Pourmand, N.; Webb, C. D.; Davis, R. W.; Yasuda, K.; Karhanek, M. Current Rectification with Poly-L-lysine-Coated Quartz Nanopipettes. *Nano Lett.* **2006,** *6*, 2486–2492.
32. Karhanek, M.; Kemp, J. T.; Pourmand, N.; Davis, R. W.; Webb, C. D. Single DNA Molecule Detection Using Nanopipettes and Nanoparticles. *Nano Lett.* **2005,** *5*, 403–407.